



Comparative study of the mesostructure of natural and synthetic polyisoprene by size exclusion chromatography-multi-angle light scattering and asymmetrical flow field flow fractionation-multi-angle light scattering

Stéphane Dubascoux^{a,*}, Chalao Thepchalerm^{a,b,f}, Eric Dubreucq^a, Suwaluk Wisunthorn^c, Laurent Vaysse^d, Suda Kiatkamjornwong^e, Charoen Nakason^b, Frédéric Bonfils^{f,**}

^a Montpellier SupAgro, UMR IATE 1208, 2 Place Viala, 34060 Montpellier, France

^b Center of Excellence in Natural Rubber Technology, Faculty of Science & Technology, Prince of Songkla University, Pattani Campus, Pattani, Thailand

^c Faculty of Science and Industrial Technology, Prince of Songkla University, Surat Thani Campus, Surat Thani, Thailand

^d CIRAD, UMR IATE 1208, KU-CIRAD Laboratory, Agroindustry Building 3, 7th Floor, Kasetsart University, Bangkok 10900, Thailand

^e Faculty of Science, Chulalongkorn University, Bangkok, Thailand

^f CIRAD, UMR IATE 1208, 2 Place Viala, 34060 Montpellier, France

ARTICLE INFO

Article history:

Received 8 July 2011

Received in revised form

18 November 2011

Accepted 1 December 2011

Available online 9 December 2011

Keywords:

Field flow fractionation

Size exclusion chromatography

Polyisoprene

Multi angle light scattering

Rubber

ABSTRACT

This paper presents results from the first analyses of the mesostructure of natural rubber (NR) by asymmetrical flow field flow fractionation (AF4). The results are compared with those obtained by size exclusion chromatography (SEC) in terms of average molar masses, radius of gyration and insoluble part (or gel quantity). Comparable results were obtained for the sample not containing gel. Conversely, for samples with gel, significant differences were found due to the presence of microaggregates. Contrary to SEC, AF4 fractionation enables partial fractionation of polyisoprene chains and microaggregates in a single run without preliminary treatment. The results presented here also highlight the special structure (very compact spheres) of microaggregates in NR compared to chemical crosslinked microaggregates in synthetic polyisoprene. The advantages and drawbacks of both techniques for analysing NR samples are also discussed.

© 2011 Elsevier B.V. All rights reserved.

1. Introduction

For natural rubber (NR), as for numerous biopolymers, it is rather simplistic to speak about macromolecular structure. Indeed, biopolymers often exhibit a complex associative structure, a mixture of macromolecular chains, microaggregates and macroaggregates [1,2]. Because of that, the term mesoscopic structure or mesostructure, which includes both macromolecular structure and aggregate characterization, is increasingly being used. Although NR mesostructure has been studied for many years, the origins of its unique properties are not yet fully clear. Recently, Kim et al. [3,4] revisited the mesostructure of NR. They [3,4] analysed NR samples with SEC-MALS and showed that the soluble part injected into a SEC system contained very few branched macromolecules, contrary to earlier published studies [5–7]. It was shown [3,4] that the soluble

part of NR in solution in tetrahydrofuran (THF) was composed of a mixture of linear chains and assumed compact microaggregates ($R_g \approx 110\text{--}130\text{ nm}$) [3,4]. They argued that to more effectively ascertain the mesostructure of NR, as is the case with most polymers, a MALS detector coupled with SEC is required. From a mechanistic point of view, many mechanisms have been proposed to explain the associative structure of NR [8–11]. The most recent proposal is Tanaka's group scheme involving a protein and a phospholipid at each end of the poly(*cis*-1,4-isoprene) chain. These two reactive end chains would appear to be involved in what they called the "naturally occurring network" of NR [12,13].

Today, many tools are available for macromolecule analysis. Of these techniques, size exclusion chromatography (SEC) and field flow fractionation (FFF) are tools of choice to fractionate macromolecules according to their sizes. SEC is beyond doubt the most popular and developed technique for polymer separation. However, a recent study has also highlighted some difficulties for NR separation with SEC coupled with a multi-angle light scattering (MALS) detector because of an abnormal elution phenomenon [3]. This abnormal elution is most likely due to co-elution of microaggregates with short chains. Kim et al. [3] showed that the abnormal

* Corresponding author. Tel.: +33 0499613016.

** Corresponding author. Tel.: +33 0499612410.

E-mail addresses: stephane.dubascoux@supagro.inra.fr (S. Dubascoux), frederic.bonfils@cirad.fr (F. Bonfils).

elution occurring with NR could be overcome by treating the SEC columns with an ionic surfactant. After treatment, it was possible to separate these compact microaggregates from linear random coil polyisoprene chains [3]. However, it is difficult to be sure whether or not all microaggregates elute and the procedure is rather cumbersome. The solution to this SEC limitation for NR sample analysis might be the use of techniques based on field flow fractionation. Recent reviews have demonstrated the potentiality of FFF in various fields, such as polymers [14], biomolecules [15], nanoparticles [16] or environment [17]. Similar to SEC, FFF could easily be coupled on-line with different detectors, such as a refractive index detector, an ultra-violet detector, a light scattering detector or an inductively coupled plasma mass spectrometer [18,19]. Recent works, emphasized the fact that field flow fractionation techniques can provide effective separation of polymer and microgel [14], or better characterization of branched ultrahigh molar mass polymers [20]. The most popular FFF techniques used for polymer fractionation are thermal flow field flow fractionation (Th-FFF) and Flow Field Flow Fractionation (FI-FFF or F4) [14]. The main difference between these two sub-techniques is the field used for the fractionation. Fractionation takes place in a channel and the field is a thermal gradient for Th-FFF, while it is a crossflow stream carried through an ultrafiltration membrane in the case of FI-FFF [21]. Up to now, only Th-FFF has been used for NR characterization [22–25]. However, during Th-FFF, macromolecules are separated according to their size and their chemical composition. Thus, heterogeneity in the chemical composition of a given polymer can complicate the determination of macromolecular structure. Asymmetrical FI-FFF (AsFI-FFF or AF4) is FI-FFF where the channel is semi-permeable and asymmetric, involving less sample dilution [21]. Natural rubber has been analysed by Th-FFF using either the polyisoprene calibration curve [22,24,25] or a multiangular light scattering detector (MALS) [23]. Lee and Molnar [25] compared the analysis of natural rubber by Th-FFF and SEC. They used a calibration curve made with linear standards poly(*cis*-1,4-isoprene). The analysed NR samples (RSS1 type) had a number-average molar mass (M_n) of about 0.8 million g mol^{-1} and a weight-average molar mass (M_w) of about 29 million g mol^{-1} , M_w being three times higher than that given by SEC. Lee and Molnar [25] showed that the high molar masses and microgels disappeared after mastication of a NR sample in an extruder. The range of molar masses found was between 10,000 and 10 million g mol^{-1} (non-masticated RSS). Filtration of the solution through filters with 5 μm pores led to a shift in the fractogram towards lower retention times. This phenomenon was observed for non-masticated rubber but not for masticated rubber. This shift to lower molar masses was attributed to the removal and/or degradation of microgels (or ultra-high molar mass species). They quantified the gel rate (as a % of total rubber, w/w) in the NR samples by Th-FFF and found slightly lower values (RSS 13%, masticated RSS 0%) than with their conventional method – i.e. filtration through a 125 μm wire mesh after 24 h in toluene (RSS 15%, masticated RSS 0%). Fulton [23] analysed two synthetic polyisoprenes (IR305, Natsyn2200), a polybutadiene (Europrene BR40) and a natural rubber (SMR5L) in cyclohexane by Th-FFF-MALS without any filtration. They showed that the IR305 sample was essentially linear with no gel, as confirmed later by Kim et al. [3] by SEC-MALS, contrary to the Natsyn2200 sample, which had a 25% gel rate and was branched for molar masses above $5 \times 10^5 \text{ g mol}^{-1}$. While there was no steric effect in the separation process for the two synthetic polyisoprenes, they observed such an effect for the polybutadiene and the NR samples. As a consequence of this phenomenon, very large entities eluted together with the smaller molecules. Bang et al. [26] used AF4 to characterize and determine the molar mass distribution of styrene-butadiene rubber.

This paper presents the first study of synthetic and natural polyisoprene fractionation by AF4 coupled with MALS in an organic

solvent (tetrahydrofuran). The peak shape is discussed and the results in terms of average molar masses, radius of gyration and gel content are compared with those obtained by SEC-MALS. The comparison of AF4-MALS with SEC-MALS also made it possible to evaluate the discrepancies between the two techniques for analysing NR samples.

2. Materials and methods

2.1. Samples

In order to compare SEC and AF4 results on synthetic polyisoprene and natural rubber (NR), four samples were chosen for their differences in mesostructure. The two synthetic poly(*cis*-1,4-isoprenes) were Kraton IR 307 (Kraton polymer, Houston, USA) and Nippol 2200 (Zeon Corporation, Louisville, USA). The main difference between these two synthetic polyisoprenes is the gel rate: no gel in the IR307 sample and presence of microgel in Nippol 2200. The two natural rubbers, M160 and M121, were TSR5CV (Technically Specified Rubber with a Constant Viscosity) made from monoclonal *Hevea brasiliensis* latex. The preparation of the samples was described previously [27].

In order to reach a sample concentration of 1 mg mL^{-1} , $30 \pm 5 \text{ mg}$ of the samples was dissolved in about 30 mL of HPLC grade tetrahydrofuran (THF, VWR, West Chester, USA) stabilized with 2,6-di-*tert*-butyl-4-methylphenol – BHT (Sigma-Aldrich, Saint Louis, USA) at 250 mg L^{-1} . The flasks were precisely weighed ($\pm 0.01 \text{ mg}$) before and after filling with THF to determine the exact concentration of the solutions. The solvent (THF+BHT) was filtered at 0.1 μm before use. Each sample was analysed in triplicate to evaluate measurement repeatability. All solutions were stored in the dark in a water bath at 30°C for 7 days and gently shaken at 30 rpm (rotational agitator REAX 2, Heidolph, Schwabach, Germany) for 1 h each day for optimum dissolution. Before injection, the macrogel and part of the microgels were removed from all the solutions by filtration at a 1 μm cutoff with Acrodisc glass filters (Pall, Port Washington, USA) to avoid both clogging of the column during SEC analysis and a steric effect (resulting in inverse elution) on AF4 fractionation [23]. For NR, the gel rate has often been determined by gravimetry, after centrifugation, and is usually called the “macrogel” or “gel phase.” Microaggregates fraction, usually called “microgel,” remaining in solution after centrifugation [28,29].

Two monodisperse polystyrene standards at 200 and 1460 kg mol^{-1} from Polymer Standard Service (PSS, Mainz, Germany) were used to assess the quality of the separation/fractionation and detector response for each SEC/AF4 injection series.

2.2. AF4 experiments

The AF4 system was a Postnova AF2000 MT series (Postnova Analytics GmbH, Landsberg, Germany) equipped with a channel adapted for organic solvents and a 350 μm spacer. The membrane was made of cellulose material treated for compatibility with organic solvents with a cut-off of 5 kg mol^{-1} (Postnova Analytics GmbH, Landsberg, Germany). The temperature setpoint of the AF4 oven containing the channel was 45°C . The detector flow was kept constant at 0.65 mL min^{-1} . The focusing step consisted of a flow delivered by the injection port of about 0.2 mL min^{-1} with a cross-flow of 1 mL min^{-1} for 6 min. Then, a 1 min transition time was applied to avoid a major pressure drop during the switch from the focus step to the elution step. The elution program is given in Table 1.

An autosampler (PN 5300 model, Postnova Analytics GmbH) was used to carry out the 100 μL sample injections.

Table 1
AF4 crossflow programme during elution.

| Step | Duration (min) | Crossflow (mL min ⁻¹) | Type of rate |
|------|----------------|-----------------------------------|--------------|
| 1 | 1.5 | 1 | Constant |
| 2 | 30 | From 1 to 0.08 | Linear |
| 3 | 9 | 0.08 | Constant |
| 4 | 7 | 0 | Constant |

Detection was carried out with a 7-angle multi-angle light scattering detector (PN 3070 model, Postnova Analytics GmbH) in line with a refractive index detector (2414 model, Waters Corporation, Milford, USA). The data gathered were processed with AF2000 software (Postnova Analytics GmbH) after blank subtraction for the DRI signal (used as a concentration detector) and according to the Berry model with 2nd order polynomial formalism. In fact, it has been shown that this formalism is well adapted for entities with a radius up to 50 nm [30]. As the refractive index detector signal changes during transition steps due to the AF4 functioning principle, five blank (mobile phase) injections were carried out in each injection series. The refractive index detector signal from the blank injections was subtracted for each sample injected.

For one series, each sample triplicate was injected once. Two series were carried out (i.e. a total of 6 injections was carried out for each sample) with different operators in order to evaluate the reproducibility of the analysis. Prior to each series of injections, the membrane was replaced and the detector was recalibrated with a polystyrene of molar mass 30 kg mol⁻¹ with isotropic diffusion (PSS, Mainz, Germany).

2.3. SEC experiments

The SEC system was based on an on-line ERC 3112 degaser (ERC, Saitama, Japan), a Waters 515 pump (Waters Corporation, Milford, USA). The columns, maintained at 45 °C were two Waters HMW6E (porosity 20 μm, 300 mm × 7.8 mm I.D.) plus one PLgel MIXED-A column (porosity 20 μm, 300 mm × 7.8 mm I.D.) from Varian (Varian, Walnut Creek, USA). The detectors were an 18-angle multi-angle light scattering detector (Dawn DSP model, Wyatt Technology, Santa Barbara, USA) and a refractive index detector (Optilab rEX model, Wyatt Technology). Data from angles 5 to 16 were collected and processed with Astra software version 5.3.1 (Wyatt Technology) according to the Berry method with a 2nd order polynomial model. Similarly to the AF4 injection series, each sample triplicate was injected once. Two series were carried out (i.e. a total of 6 injections carried out for each sample).

3. Theory/calculation

3.1. Light scattering theory

For the Berry method with a 2nd order polynomial fit, $[Kc/\Delta R(\theta)]^{1/2}$ is plotted against $\sin^2(\theta/2)$. According to the light scattering theory, this plot makes it possible to determine M_{wi} and R_{gi} for each slice (i) of the fractogram from AF4 or the chromatogram from SEC, respectively, according to Eq. (1).

$$\left[\frac{Kc}{\Delta R(\theta)} \right]_i^{1/2} = \left[\frac{1}{M_{wi}} + \frac{16\pi^2}{3\lambda_0^2} \frac{(R_g^2)_t}{M_{wi}} \sin^2 \left(\frac{\theta}{2} \right) \right]^{1/2} \quad (1)$$

where K is an optical constant, c is the solute concentration (in g mL⁻¹); θ is the scattering angle; $\Delta(R)\theta$ is the excess Rayleigh ratio, the ratio of scattered and incident light intensity; M_{wi} is the weight-average molar mass of the solute; λ_0 is the wavelength of the laser beam in a vacuum (in nm); R_g is the gyration radius of the solute (nm).

The optical constant K is given by Eq. (2).

$$K = \frac{4\pi^2 n_0^2}{N_A \lambda_0^2} \left(\frac{dn}{dc} \right)^2 \quad (2)$$

where n_0 is the refractive index of the solvent; N_A is Avogadro's number; (dn/dc) is the differential refractive index increment of the polymer in the solvent used.

For detailed information about the light scattering theory, refer to [31,32].

3.2. Radius definitions

The radius of gyration ($\langle R_g \rangle$) or root mean square radius (r.m.s.) is defined for a non-rigid particle consisting of mass elements of mass m_i , each located at a distance r_i from the center of mass as:

$$\sqrt{\langle R_g^2 \rangle} = \frac{\sum_i m_i r_i^2}{\sum_i m_i} \quad (3)$$

3.3. Gel content calculation

In order to evaluate the amount of gel retained by the 1 μm filter, the whole peak from the concentration detector (refractive index detector) observed in SEC or AF4 separation was integrated using 0.13 mL g⁻¹ as the value of dn/dc [33]. This gel content, residue remaining on the filter, was called the “filtrate gel on 1 μm” or $Gel_{>1\mu}$. Not all authors determined the gel rate in NR by the same method and did not therefore measure the same thing. For NR, the gel rate has often been determined by gravimetry, after centrifugation, and is usually called the “macrogel” or “gel phase.” A few authors filtrated the sol fraction to determine also the microaggregates rate, usually called “microgel,” [10,28,34–36] remaining in solution after centrifugation. The total gel was given adding the macrogel and microgel rates. But as shown by Kim et al. [3], even after filtration on 1 μm porosity filters, it remains microaggregates in solution which are injected in SEC or AF4. For this reason, in this paper two different gel rate were determined (i) the “filtrate gel on 1 μm” or $Gel_{>1\mu}$, former “total gel” used in previous papers and (ii) the “filtrate gel inferior to 1 μm” or $Gel_{<1\mu}$ [3]. As a consequence, the real total gel (G_T) is:

$$G_T = Gel_{>1\mu} + Gel_{<1\mu} \quad (4)$$

$Gel_{<1\mu}$ is the quantity of microaggregates with a size smaller than 1 μm. $Gel_{<1\mu}$ cannot be determined by SEC-MALS, except by treating the columns with tetrabutylammonium bromide (TBABr) as shown previously [3]. This procedure is rather cumbersome, whereas it will be shown that $Gel_{<1\mu}$ can easily be estimated using AF4 analysis of NR samples. Indeed, by knowing the initial concentration of the sample before filtration, it is possible to determine from the fractogram (DRI signal) the concentration of the two populations in solution after filtration: polyisoprene chains and microaggregates smaller than 1 μm. Thus:

$$Gel_{>1\mu} = 100 - \frac{C_1 \times 100}{C_0} \quad (5)$$

$$Gel_{<1\mu} = \frac{C_2 \times 100}{C_0} \quad (6)$$

where C_0 is the initial concentration of the analysed sample, C_1 the concentration of the analysed sample passing through the 1 μm filter (polyisoprene chains + microaggregates) and C_2 the concentration of only the microaggregates passing through the 1 μm filter. C_1 can be determined either by SEC or AF4 by integrating the whole peak of the concentration detector (DRI). C_2 can be calculated only by AF4 integrating the part of the DRI peak containing microaggregates.

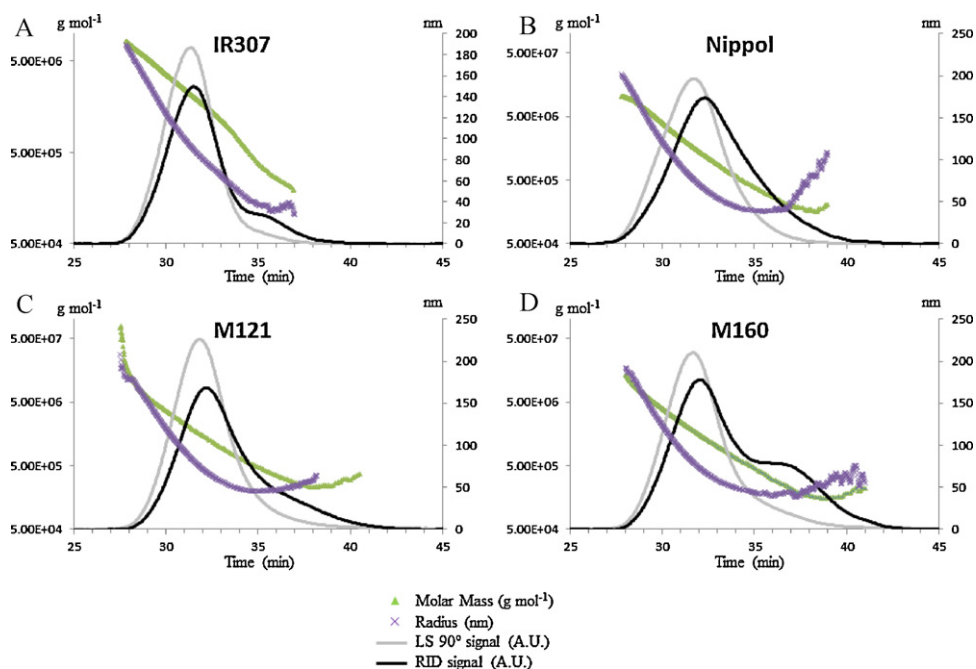


Fig. 1. Chromatograms (from the RID and LS detector at 90°) and variation in R_{gi} and M_{wi} depending on the elution time during SEC analysis.

All calculations of the concentration were realized using a dn/dc corresponding to the one of polyisoprene (equal to 0.13 mL g^{-1}) [33]. Indeed, the dn/dc of micro-aggregates is assumed to be close of polyisoprene one as there are mainly constituted of polyisoprene.

4. Results and discussion

4.1. Qualitative description of fractograms

SEC-MALS profiles for the different samples are presented in Fig. 1. M_{wi} variations started with a linear decrease corresponding to a normal elution from large chains to small chains but displayed a deviation of the slope of this curve for samples containing gel (i.e. Nippol, M121 and M160, Fig. 1B–D). As described in the introduction and as previously detailed [3], SEC separation of rubber generally presents this abnormal elution due to co-elution of delayed large macromolecules, assumed to be microaggregates ($Gel_{<1\mu}$), with the small chains of poly(*cis*-1,4-isoprene). This particular elution was highlighted when either a change or an inversion of the slope presenting the variation in weight-average molar mass versus elution volume occurred. Regarding the detectors, the differential refractive index (DRI) signal during the SEC elution profile corresponded to a main Gaussian peak (with slight back-tailing) for Nippol and M121, and to a bimodal molar mass distribution for the IR307 and M160 samples. The LS signal was more unimodal with back-tailing varying depending on the sample.

Unlike SEC, AF4 fractionated the macromolecules from small to large ones and the peak shapes appeared quite different. For poly(*cis*-1,4-isoprene) with gel (i.e. Nippol 2200, M160 and M121), the shape of the LS fractograms did not correspond to a Gaussian peak. The fractograms displayed a long front tailing (i.e. a long and low signal increase) and an abrupt increase in the LS signal from 25 to 30 min (corresponding to a crossflow ranging from 0.5 to 0.3 mL min^{-1}) (Fig. 2). For the IR307 sample, the fractogram exhibited a clearly less pronounced increase in the LS signal (Fig. 2A). As the IR307 sample did not contain gel, unlike the Nippol 2200 sample, this abrupt increase in the signal was due to microaggregates, as observed by Andersson et al. [37] for AF4 analysis of ethylhydroxyethyl cellulose. For the refractive index detector signal, the

behaviour was unfamiliar, with a first peak close to void volume (elution starting at 7 min), corresponding to small chains, followed by either a slight increase in the concentration signal (for IR 307), or a decrease (for Nippol 2200), or quite a constant signal up to the end of the peak (for the two natural samples) (Fig. 2).

For natural rubber samples analysed by SEC-MALS, Kim et al. [3] showed a clear separation of two populations (random coil and compact micro-aggregates sphere like) after treatment of columns with an ionic surfactant.

In Fig. 2, the fractograms (from LS and DRI detectors) did not give a clear separation (bimodal) of the two entities eluting, but presented a continuous elution with evenly increasing molar mass starting from relatively small molecules towards high/ultra-high molar masses and probably the compact micro-aggregates. However, the evolution of the molar masses (M_{wi}) in line with the elution time was not linear from a qualitative viewpoint (Fig. 2). For the IR307 sample, Fig. 2A shows a change in slope for an elution time of 17–18 min ($M_{wi} \approx 600 \text{ kg mol}^{-1}$). A clear decrease in the variability of the measured R_{gi} was observed from this elution time ($t_e = 17\text{--}18 \text{ min}$) (Fig. 2). Indeed, for the first 18 min of the fractogram, R_{gi} values were very dispersed whatever the samples analysed using Berry 2 formalism (Fig. 2), compared to SEC-MALS. This high dispersion of R_{gi} may have occurred because the concentrations of the injected solutions were too low ($\approx 1 \text{ mg mL}^{-1}$) for LS detection or because there was a lack of resolution for small molecule fractionation under our AF4 conditions. This initial slope change in M_{wi} was observed for other samples at times that varied depending on the sample (from 13 up to 17 min). With the Nippol sample, a second marked change appeared in the M_{wi} slope at an elution time of about 31 min (Fig. 2B). This abrupt slope change was accompanied by a dramatic increase in the LS signal due to huge entities eluting ($250 < R_{gi} < 1000 \text{ nm}$). Though the size determination by MALS of structures close to 1000 nm (for Nippol sample) is highly questionable and usually prone to large errors, this second change in the M_{wi} slope in line with the elution time was not visible for the other synthetic polyisoprene (IR307), but was visible to a lesser extent (lower radius of gyration) for the two NR samples (M121 and M160) at an elution time of about 26–27 min (Fig. 2C and D).

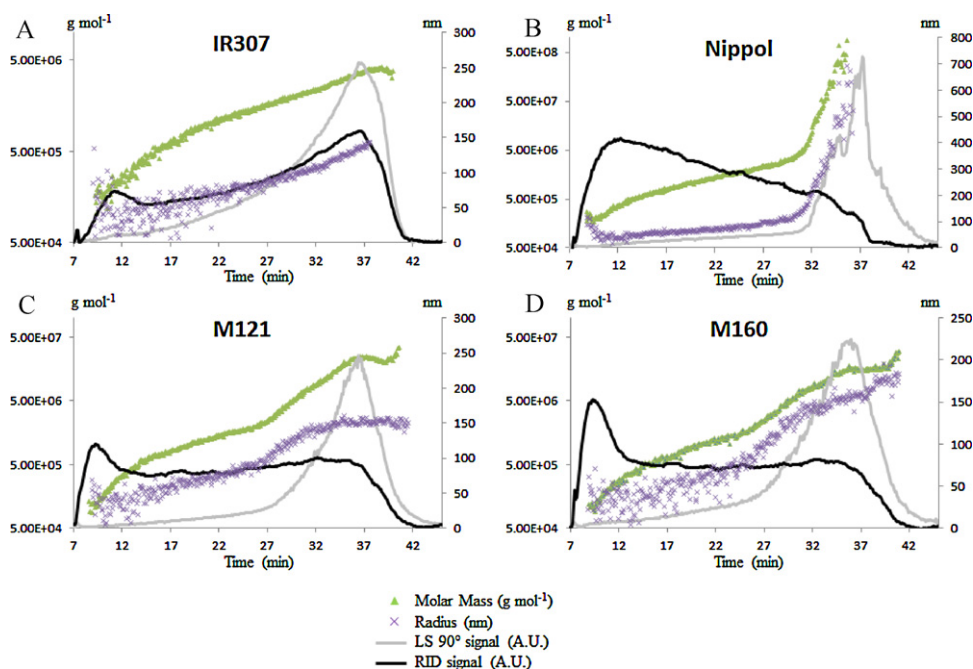


Fig. 2. Fractograms (from the RID and LS detector at 90°) and variation in R_{gi} and M_{wi} depending on the elution time during AF4 analysis.

The molar mass distribution (MMD) from AF4 separation for IR 307 confirmed the presence of only one population of chains with a M_{wi} ranging from about 60 000 g mol^{-1} to about 10 million g mol^{-1} (Fig. 3A). Conversely, the MMD from AF4 separation for the Nippol clearly showed the presence of 2 distinct populations (Fig. 3A). The first population, centered to about 800 kg mol^{-1} was probably composed exclusively of isolated polyisoprene chains and the second one, centered to about 400 million g mol^{-1} , composed of microaggregates. For the two NR samples (M121 and M160) (Fig. 3B), the MMD from AF4 separation clearly show also two populations: isolated polyisoprene chains ($20 < M_{wi} < 3000 \text{ kg mol}^{-1}$) and microaggregates ($3 < M_{wi} < 40 \text{ million g mol}^{-1}$). As previously stated, it can be noticed on the AF4 separation profiles for natural polyisoprene an increase in the $M_{wi} = f(V_e)$ and $R_{gi} = f(V_e)$ slopes between 26 and 27 min according to the sample (Fig. 2C and D). These increases in the slopes are most probably due to the elution of microaggregates. After this elution time, the M_{wi} profile exhibited an increase in slope (from 27 to about 35 min), reaching a quasi-plateau (from 35 min). This behaviour suggests that this population was quite monodisperse. These two parts could be attributed to co-elution of isolated polyisoprene chains and $\text{Gel}_{<1\mu}$ in the first case and $\text{Gel}_{<1\mu}$ only for the plateau.

Large differences were observed for the $M_{wi} = f(V_e)$ and $R_{gi} = f(V_e)$ slopes, the sizes (R_{gi}) and the molar masses (M_{wi}) of the second populations for Nippol compared to the two natural polyisoprene samples (Fig. 2). These results tend to confirm that the gel was not intrinsically the same for natural and synthetic polyisoprene. Indeed for NR, the radius for the $\text{Gel}_{<1\mu}$ was about 150 nm for a molar mass close to 15 million g mol^{-1} whereas for Nippol for the same molar mass the radius was about 240 nm (i.e. 60% higher), as illustrated in Fig. 4. Moreover, there was no “plateau effect” for Nippol compared to the NR samples. In addition, Fig. 5 shows that the distribution range of the R_{gi} for the natural polyisoprene samples (M121 and M160) is very close to the distribution of the R_{gi} for IR307 sample. Thus, with a lower R_{gi} for the same M_{wi} , the microaggregates in the NR samples seemed more compact than in the Nippol synthetic polyisoprene. However, some of the difference observed in the slopes may have been due to an underestimation of M_{wi} for the microaggregates of the NR samples. Indeed, it

cannot be ruled out that the dn/dc of NR microaggregates is not constant. Changes in the non-isoprene composition (lipids and/or proteins) of microaggregates cannot be excluded. A change in the proportion of non-isoprene compounds versus polyisoprene in the

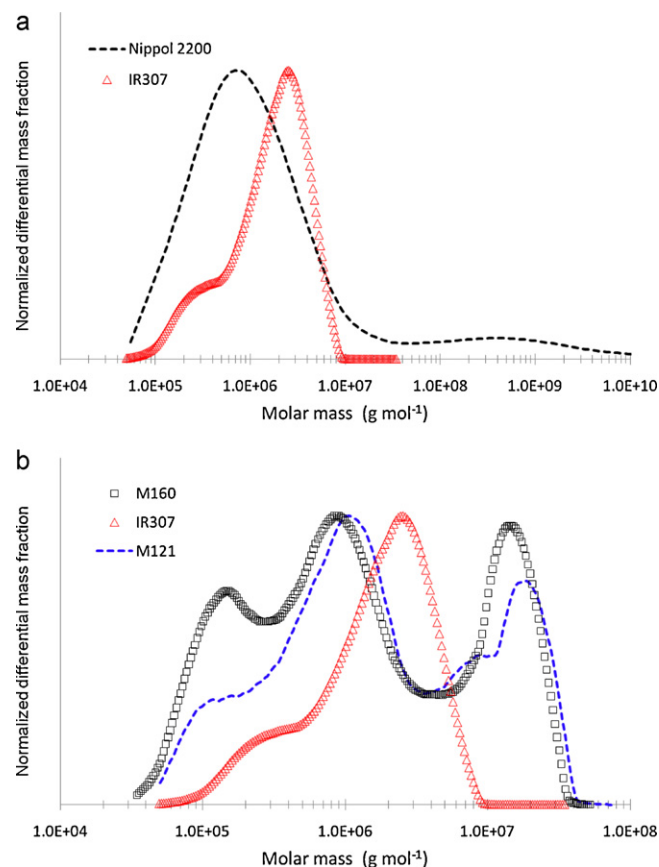


Fig. 3. Molar mass distribution from AF4 separation for (A) the two synthetic polyisoprene samples (IR2200 and IR307) and (B) the two natural polyisoprene samples (M160 and M121) compared to IR307.

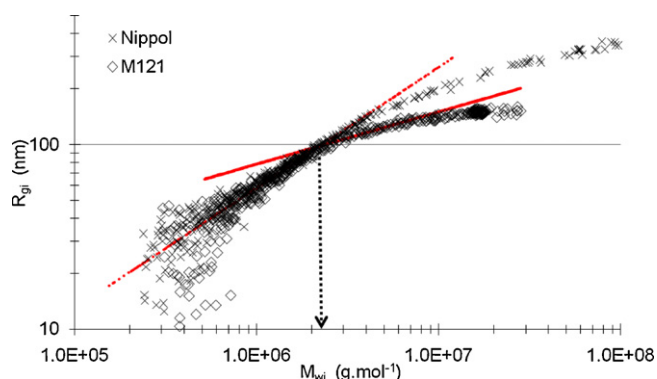


Fig. 4. Variation of the radius of gyration (R_{gi}) depending on molar masses (M_{wi}) for the Nippol 2200 and M121 samples (for M121, model 1: $R_{gi} = 0.007 \times M_{wi}^{0.653}$, model 2: $R_{gi} = 1.57 \times M_{wi}^{0.283}$). (For interpretation of the references to color in the text, the reader is referred to the web version of the article.)

microaggregates could lead to a change in the dn/dc and so in the M_{wi} determined.

One of the main difficulties encountered with RID hyphenated with AF4 fractionation is to define a correct and unbiased integration range. For our data, the integration range for average molar mass and radius of gyration assessment was started when the M_{wi} and R_{gi} signals were stabilized (out of void peak influence) and stopped just before the end of the peak (shown as the red box in Fig. 6 for M160, for example). This choice of integration area was made in order to have results including almost all the peak surface and to avoid a decrease in repeatability for the AF4 results due to pre- and post-peak radius and mass dispersion and heterogeneity because of a low LS signal. This method was applied for the AF4 signals from IR307, M160 and M121. On the other hand, the treatment for Nippol 2200 was different. Indeed, the variation in M_{wi} in the second part of Nippol 2200 fractionation was quite high due to the presence of microaggregates with ultra-high molar masses (over 10^{10} g mol⁻¹). Moreover, this final M_w increase was quite noisy and unrepeatable, probably due to the low associated RID signal. In fact, as presented in Table 2 for example, increasing the Nippol 2200 integration range (from 9.5–35 min to 9.5–40 min), drastically increased the average molar masses, but also the standard deviation. Lastly, a 7% increase in RID integration area (hence in quantity) led to an increase of 4 orders of magnitude for the M_w and resulted in an increase in the standard deviation from 25% to 71%. Consequently, for Nippol, the integration range was shortened, compared to the other samples, to avoid excessive variability in the results.

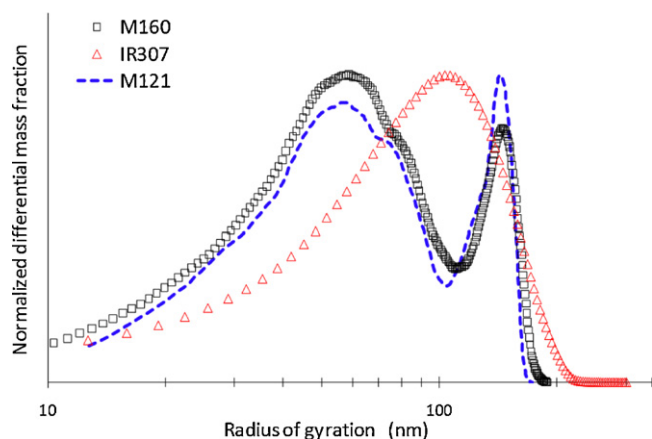


Fig. 5. Radius of gyration distribution from AF4 separation for the two natural polyisoprene samples (M160 and M121) compared to IR307 sample.

In order to quantify aggregates exceeding $1 \mu\text{m}$ ($\text{Gel}_{>1\mu}$) (estimation of C_1 in Eq. (5)), the whole peak was integrated (green box in Fig. 6). The quantity of microaggregates smaller than $1 \mu\text{m}$ ($\text{Gel}_{<1\mu}$) (estimation of C_2 in Eq. (6)) was calculated according to a third integration range (the blue box in Fig. 6) starting from the middle of the zone we considered as a mixture of polyisoprene chains and microaggregates up to the end of the peak. This start was chosen according to the M_{wi} given by the intersection of the two slopes (red lines) observed in Fig. 4 (data $R_g = f(M_w)$) and corresponding to the deviation from the initial linearity (i.e. first red line in Fig. 4). Indeed, for M121 sample, the M_{wi} determined at the intersection between the two slopes (models 1 and 2, Fig. 4) allowed to determine the elution time (t_e) corresponding to the beginning of microaggregates eluting in the LS detector. The M_{wi} given by the intersection of the two models (Fig. 4) was approximately 2.2 millions g mol⁻¹ (see arrow in Fig. 4) which corresponds to an elution time of 27 min. It can be noticed in Fig. 2C (see the arrow) that this elution time corresponds to the change in the slope for $M_{wi} = f(t_e)$.

4.2. Comparison of data between SEC-MALS and AF4-MALS

4.2.1. Average molar masses

M_n , M_w and M_z were calculated from the SEC and AF4 results for each sample. The results are presented in Fig. 7.

The number average molar mass M_n did not present significant differences whether determined by SEC or AF4 (Fig. 7). The ratio of M_n obtained by AF4 to that obtained by SEC was ranged between 0.85 and 1.0. Unlike M_n , M_w and M_z were different, with a higher M_w and M_z obtained for AF4. As described previously, these larger M_w and M_z can be explained by the presence of large microaggregates not observed with SEC. This observation is confirmed by the fact that for IR 307 (poly(*cis*-1,4-isoprene) without gel), M_w and M_z exhibited no significant difference between SEC and AF4 results. The difference between AF4 and SEC in terms of average molar masses was, as expected, higher for M_z than for M_w . The M_w ratios ($M_{w-AF4}:M_{w-SEC}$) ranged from 1.0 to 4.3 (for IR 307 and M121, respectively) whereas the M_z ratios ($M_{z-AF4}:M_{z-SEC}$) ranged from 1.0 to 18.6 (for IR 307 and Nippol, respectively). For the three average molar masses considered (i.e. M_n , M_w or M_z), the AF4 results showed greater heterogeneity than for the SEC results, with high standard deviations. This lower reproducibility and repeatability was mainly due to the difficulty in defining the integration range, as previously explained, but also to the substantial variability generated by the refractive index detector baseline position. Indeed, the AF4 principle resulted in some noise, deviations and jumps in the DRI baseline and thus to some doubts/uncertainties on the baseline position, despite the blank subtraction. The large M_z difference (from AF4 to SEC) and RSD for Nippol was due to the large amount of microaggregates with ultra-high molar masses and to the poor repeatability in the high mass range, as explained later on.

4.2.2. Determination of gel rates

The gel rates in the samples were calculated after SEC and AF4 analysis. $\text{Gel}_{>1\mu}$ was calculated for both the SEC and AF4 analyses whereas $\text{Gel}_{<1\mu}$ was only calculated after AF4 analysis. Fig. 8 presents the $\text{Gel}_{>1\mu}$ rate after SEC and AF4 analyses. For the IR 307 and Nippol samples, the $\text{Gel}_{>1\mu}$ rate did not display any significant difference (no gel for IR307 and average $\text{Gel}_{>1\mu}$ slightly higher for Nippol with AF4). For the two NR samples, only M160 exhibited a significant difference in the $\text{Gel}_{>1\mu}$ rate between SEC and AF4 determination (23.8% for SEC and 17.2% for AF4). For M121, the lack of significant difference was due to the high variance of the AF4 result. The $\text{Gel}_{<1\mu}$ calculation was estimated at 9.5% for Nippol, 27% for M160 and 29% for M121 (no $\text{Gel}_{<1\mu}$ for IR 307). These large quantities of $\text{Gel}_{<1\mu}$ explained the large differences observed for

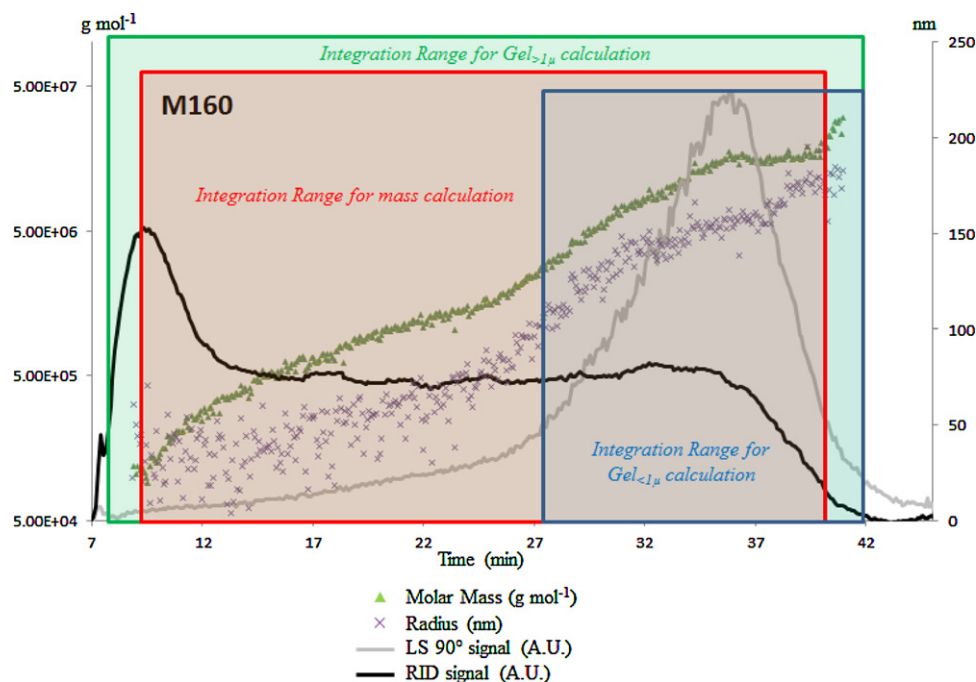


Fig. 6. Determination of the AF4 integration ranges for the M160 sample. (For interpretation of the references to color in the text, the reader is referred to the web version of the article.)

Table 2

Nippol 2200 mass calculation (M_n , M_w and M_z with respective RSD from one AF4 series) with different integration ranges.

| | integration start | integration end | M_n (Da) | RSD | M_w (Da) | RSD | M_z (Da) | RSD |
|--------------------|-------------------|-----------------|------------|-----|------------|-----|------------|-----|
| Nippol 2200 | 9.5 min | 35 min | 6.95E+05 | 4% | 3.61E+06 | 25% | 4.24E+07 | 62% |
| | 9.5 min | 40 min | 7.48E+05 | 4% | 9.36E+10 | 71% | 1.40E+14 | 81% |

Integration : +7% of surface area

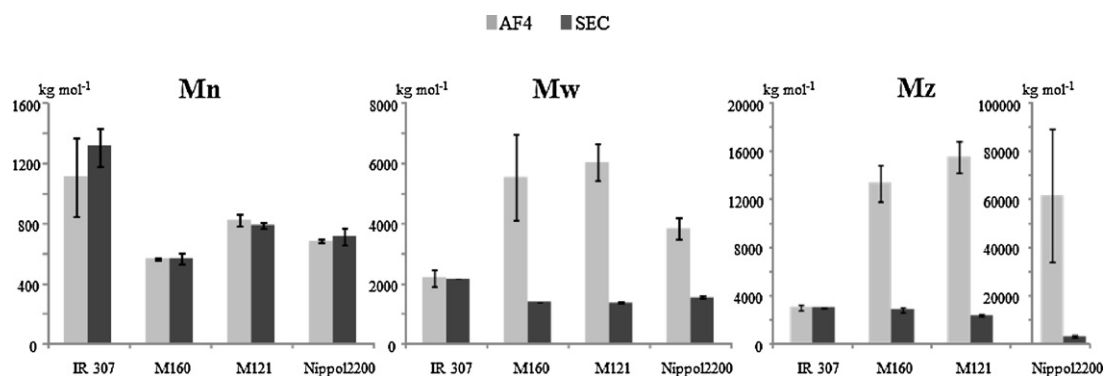


Fig. 7. Comparison of masses obtained by SEC and AF4.

M_w and M_z in the NR samples and the Nippol sample (higher M_w and M_z for AF4 analyses compared to SEC). However, as a result of such a large quantity of Gel_{<1μ} for the NR samples, assumed to be “lost” in not insubstantial proportions in SEC, the Gel_{>1μ} rate should have been much lower with AF4 compared to SEC for Nippol, M160 and M121. The slight difference observed between AF4 and SEC for the Gel_{>1μ} rate could be explained either by the large measurement variability for AF4, or by an overestimated Gel_{>1μ} calculation in AF4 analysis (potentially due to concentration peak area determination and therefore to blank subtractions). For the Gel_{<1μ} calculation, Kim et al. [3] obtained Gel_{<1μ} values close to 10% (calculated by SEC after ionic surfactant treatment of the columns) for NR samples similar to M160 and M121, meaning a difference with our Gel_{<1μ} values of about 15%.

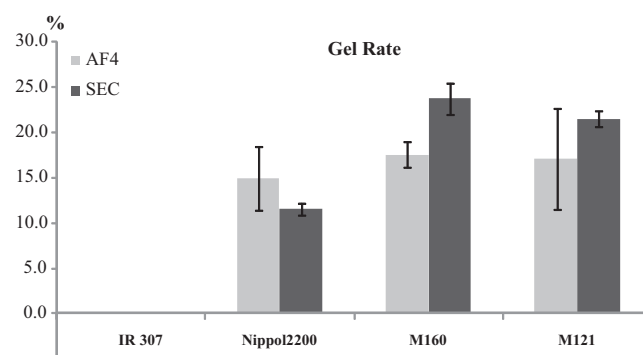


Fig. 8. Comparison of filtrate gel on 1 μm (Gel_{>1μ}) rate calculated by AF4 and SEC.

Table 3
 R_z determined by AF4 and SEC.

| | | R_z (nm) | SD (nm) ^a | CV ^a |
|--------|-----|------------|----------------------|-----------------|
| IR307 | AF4 | 115.8 | 3.8 | 4.0% |
| | SEC | 112.1 | 1.4 | 1.3% |
| Nippol | AF4 | 249.9 | 28.8 | 28.8% |
| | SEC | 108.5 | 4.2 | 3.9% |
| M160 | AF4 | 136.5 | 7.0 | 4.3% |
| | SEC | 102.8 | 2.3 | 2.2% |
| M121 | AF4 | 133.5 | 7.8 | 3.4% |
| | SEC | 92.5 | 2.4 | 2.6% |

^a SD: standard deviation, CV: coefficient of variation ((SD/mean) × 100).

4.2.3. Comparison of radii of gyration

As for the average molar masses, the R_z values obtained with AF4 were higher than those obtained with SEC, except for the IR307 sample, whose R_z was the same for both separation techniques (see Table 3). Nevertheless, the differences in R_z obtained with the two techniques were less pronounced than for M_z . This was due to the narrower radius of gyration size range observed (typically varying from 20 to 200 nm) compared to the 10^2 – 10^3 order of magnitudes for the masses over the whole fractionation (up to 10^5 for Nippol). The variation in R_{gi} depending on the elution time with AF4 displayed a similar behaviour to that for M_{wi} (Fig. 2). As the variation in R_{gi} was less significant than for M_{wi} , it implies that the material was becoming increasingly compact (greater increase for masses than for radii) towards the end of the elution, especially for the second population, as previously illustrated in Fig. 4. This observation confirms the presence of compact microaggregates highlighted by Kim et al. [3].

5. Conclusions

This work demonstrates the ability of AF4 to fractionate natural and synthetic poly(*cis*-1,4-isoprene). Distinct populations (characterized by a clear slope change in M_{wi} variation and by the slope change in the conformation plot) corresponding to isolated polyisoprene chains and microaggregates smaller than 1 μm ($\text{Gel}_{<1\mu}$) were detected. Average molar masses were determined and compared with those obtained by SEC. Similar M_n values were obtained but large differences were observed for M_w and M_z . These differences could be explained by a microgel population observed in AF4 but not during SEC separation. Moreover, microaggregates in the NR samples exhibited quite a different structure, appearing more compact than the microaggregates in the Nippol synthetic polyisoprene. Some problems (difficulties in defining the baseline, DRI signal jumps, etc.) due to the use of DRI with AF4 were encountered, in particular for gel rate determination. It seems obvious that some analytical developments are needed to optimize fractionation, increase the resolution for small polyisoprene chains and enable better reproducibility. However, these results are promising and microgel ($\text{Gel}_{<1\mu}$) can be considered for further individual studies and physico-chemical characterization.

Acknowledgements

The authors gratefully thank Emilie Croizat and Christine Char for their valuable contribution to this project. A4F-MALS and SEC-MALS analyses were carried out on the LipPol-Green platform (<http://www.supagro.fr/plantlippol-green/>). We kindly thank CIRAD DRS and Agropolis foundation (<http://http://www.agropolis-fondation.fr>) for financial support, and the Hubert Curien Programme for funding Miss Chalao Thepchalerm's scholarship.

References

- [1] H. Liu, F. Xie, L. Yu, L. Chen, L. Li, *Prog. Polym. Sci.* 34 (2009) 1348.
- [2] L. Vaysse, F. Bonfils, P. Thaler, J. Sainte Beuve, in: D.R. Höfer (Ed.), *Sustainable Solutions for Energy Generation*, Royal Society of Chemistry, Cambridge, 2009, p. 335.
- [3] C. Kim, M. Morel, J. Sainte Beuve, A. Collet, S. Guilbert, F. Bonfils, *J. Chromatogr. A* 1213 (2008) 181.
- [4] C. Kim, J. Sainte Beuve, S. Guilbert, F. Bonfils, *Eur. Polym. J.* 45 (2009) 2249.
- [5] J.L. Angulo-Sanchez, P. Caballero-Mata, *Rubber Chem. Technol.* 54 (1981) 34.
- [6] K.N.G. Fuller, W.S. Fulton, *Polymer* 31 (1990) 609.
- [7] J. Tangpakdee, Y. Tanaka, *J. Rubber Res.* 1 (1998) 14.
- [8] S.N. Gan, *J. Membr. Sci. Pure Appl. Chem. A* 33 (1996) 1939.
- [9] J. Tangpakdee Sakdapipanch, T. Kowitteeawut, K. Suchiva, Y. Tanaka, *Rubber Chem. Technol.* 72 (1999) 712.
- [10] F. Ngolemasango, E. Ehabe, C. Aymard, J. Sainte-Beuve, B. Nkouonkam, F. Bonfils, *Polym. Int.* 52 (2003) 1365.
- [11] Y. Tanaka, L. Tarachiwin, *Rubber Chem. Technol.* 82 (2009) 283.
- [12] S. Amnuaypornsi, J. Sakdapipanch, S. Toki, B.S. Hsiao, N. Ichikawa, Y. Tanaka, *Rubber Chem. Technol.* 81 (2008) 753.
- [13] J. Carretero-Gonzalez, T.A. Ezquerro, S. Amnuaypornsi, S. Toki, R. Verdejo, A. Sanz, J. Sakdapipanch, B.S. Hsiao, M.A. Lopez-Manchado, *Soft Matter* 6 (2010) 3636.
- [14] F.A. Messaud, R.D. Sanderson, J.R. Runyon, T. Otte, H. Pasch, S.K.R. Williams, *Prog. Polym. Sci.* 34 (2009) 351.
- [15] R. Qureshi, W. Kok, *Anal. Bioanal. Chem.* 399 (2011) 1401.
- [16] G. Lespes, J. Gigault, *Anal. Chim. Acta* 692 (2011) 26.
- [17] L.J. Gimbert, K.N. Andrew, P.M. Haygarth, P.J. Worsfold, *Trends Anal. Chem.* 22 (2003) 615.
- [18] S. Dubascoux, I. Le Hecho, M. Hasselov, F. Von der Kammer, M.P. Gautier, G. Lespes, *J. Anal. At. Spectrom.* 25 (2010) 613.
- [19] S. Dubascoux, F. Von Der Kammer, I. Le Hécho, M.P. Gautier, G. Lespes, *J. Chromatogr. A* 1206 (2008) 160.
- [20] T. Otte, H. Pasch, T. Macko, R. Brull, F.J. Stadler, J. Kaschta, F. Becker, M. Buback, *J. Chromatogr. A* 1218 (2011) 4257.
- [21] M.E. Schimpf, K.D. Caldwell, G.J.C. Field, *Flow Fractionation Handbook*, Wiley Interscience, 2000.
- [22] W.-S. Kim, C.H. Eum, A. Molnar, J.-S. Yu, S. Lee, *Analyst* 131 (2006) 429.
- [23] W.G. Fulton, *SA J. Nat. Rubber Res.* 12 (1997) 154.
- [24] S. Lee, C. Eum, A. Plepys, *Bull. Kor. Chem. Soc.* 21 (2000) 69.
- [25] S. Lee, A. Molnar, *Macromolecules* 28 (1995) 6354.
- [26] D.Y. Bang, D.Y. Shin, S. Lee, M.H. Moon, *J. Chromatogr. A* 1147 (2007) 200.
- [27] C. Kim, M. Morel, J. Sainte Beuve, S. Guilbert, F. Bonfils, *Polym. Eng. Sci.* 50 (2010) 240.
- [28] F. Bonfils, A. Doumbia, C. Char, J. Sainte Beuve, *J. Appl. Polym. Sci.* 97 (2005) 903.
- [29] S. Wisunthorn, S. Liengprayoon, L. Vaysse, J. Sainte Beuve, F. Bonfils, *J. Appl. Polym. Sci.*, in press.
- [30] M. Andersson, B. Wittgren, K.G. Wahlund, *Anal. Chem.* 75 (2003) 4279.
- [31] I. Teraoka, *Polymer Solutions: An Introduction to Physical Properties*, John Wiley & Sons, New York, 2002.
- [32] P.J. Wyatt, *Anal. Chim. Acta* 272 (1993) 1.
- [33] C. Kim, A. Deratani, F. Bonfils, *J. Liq. Chromatogr. Relat. Technol.* 33 (2010) 37.
- [34] D.S. Campbell, K.N.G. Fuller, *Rubber Chem. Technol.* 57 (1984) 104.
- [35] K.N.G. Fuller, *Natural Rubber Science and Technology*, Oxford University Press, 1988.
- [36] M.M. Rippel, C.A.P. Leite, L.T. Lee, F. Galembeck, *Colloid Polym. Sci.* 283 (2005) 570.
- [37] M. Andersson, B. Wittgren, K.G. Wahlund, *Anal. Chem.* 73 (2001) 4852.